Journal of Power Sources 206 (2012) 153–160

Contents lists available at SciVerse ScienceDirect

Journal of Power Sources

journal homepage: www.elsevier.com/locate/jpowsour

Absolute permeability and Knudsen diffusivity measurements in PEMFC gas diffusion layers and micro porous layers

Lalit M. Pant[a,b], Sushanta K. Mitra[a], Marc Secanell[b,*]

[a] Micro and Nano Scale Transport Laboratory, Department of Mechanical Engineering, University of Alberta, Edmonton, AB, Canada T6G 2G8
[b] Energy Systems Design Laboratory, Department of Mechanical Engineering, University of Alberta, Edmonton, AB, Canada T6G 2G8

ARTICLE INFO

Article history:
Received 10 October 2011
Received in revised form 13 January 2012
Accepted 14 January 2012
Available online 25 January 2012

Keywords:
PEM fuel cell
Absolute permeability
Knudsen diffusivity
Darcy's law

ABSTRACT

A novel approach for predicting absolute permeability and effective Knudsen diffusivity values in gas-diffusion-layers/microporous layers (GDLs/MPLs) is proposed. A conventional diffusion bridge setup with modifications is used to obtain the pressure drop across the GDL at several mass flow rates. The experimental results are then fitted to both the Darcy's model and the binary friction model (BFM). Experimental data obtained using different working gases, e.g. O_2, N_2, He and Ar, are used to validate the two model predictions. Experimental results show that the traditionally used Darcy's law is not able to predict the pressure drop across the GDL, especially in a GDL with an MPL, due to Knudsen effects. The BFM accounts for both viscous and Knudsen transport and it is thereby shown to provide more accurate predictions for any working fluid tested. Permeability and effective Knudsen diffusivities obtained using both Darcy's model and BFM for a SGL (Weisbaden, Germany) SIGRELET 34BA and 34BC are reported.

1. Introduction

Polymer electrolyte fuel cells (PEFCs) are promising energy conversion devices for applications such as automobiles, forklifts and portable electronic devices due to their high efficiency, quick start-up and zero emissions when fuelled with hydrogen. Further improvements in PEFC technology are however still needed in order to reduce cost and increase performance. Mass transport is a key process in PEMFCs, since fuel and reactants are transported to the reaction sites by convective-diffusive transport. For accurate modelling of gas transport in the fuel cell porous media, i.e. gas diffusion layers (GDLs), micro-porous layers (MPLs) and catalyst layers (CLs), a reliable set of transport properties is needed. Among the necessary parameters are gas diffusivity and permeability. Gas permeability is necessary in order to predict convective-diffusive transport inside the membrane electrode assembly or across channels [1].

Darcy's law has traditionally been used to study convective flow in porous media such as GDLs and MPLs. Darcy's law is an approximation of the Navier–Stokes equation for very low flow velocities where the flow can be assumed as a Stokes flow [2–4]. The reduced equation is volume averaged over a representative elementary volume of the porous media in order to obtain a net flow equation. The corrections for non-Stokes flows include addition of the inertial forces, also known as the Forchheimer term, and other corrections [4]. In fuel cell porous media, the convection velocities are low, hence the Stokes flow assumption can be applied.

The basic Navier–Stokes equation for gas flows is based on a continuum assumption in the flow, which is only applicable if the mean free path of the molecules is much smaller than the system length scale. For rarefied gases or at very small length scales, the number of molecules within the system length scale are not sufficient for volume averaging, and the continuum assumption breaks down. To asses the validity of the continuum approach in micro–nano pores appearing in GDLs and MPLs of a PEFC, Knudsen numbers can be used. The Knudsen number is defined as the ratio of mean free path of gas molecules to the system length scale. The pore sizes in GDLs and MPLs are within 1–150 μm [5,6] and 2–200 nm [5,7] respectively. For calculation purposes, the average pore size of a GDL can be taken as 60 μm and for an MPL as 60 nm. Table 1 shows the Knudsen number for several gases in a GDL and MPL where the mean free path for the gases was calculated at 26 °C and atmospheric pressure. The flow regime based on the Knudsen number is given in Table 2. It can be observed from Table 1 that only in the case of oxygen and nitrogen flow in the GDL, the Knudsen number is around 0.001, thereby enabling the use of Darcy's law. However, for flow in MPLs, the transport will be in the transition region, hence the use of Darcy's law might not be accurate.

As mentioned, the use of Darcy's law to estimate permeability of PEMFC porous media may be erroneous. Experimental measurements with different working fluids could be used to estimate the validity of Darcy's law. So far, very limited literature is available

* Corresponding author. Tel.: +1 780 492 6961; fax: +1 780 492 2200.
E-mail address: secanell@ualberta.ca (M. Secanell).

0378-7753/$ – see front matter © 2012 Elsevier B.V. All rights reserved.
doi:10.1016/j.jpowsour.2012.01.099

Table 1
Knudsen number calculations for different gases in GDL and MPL [19].

Parameter	PEMFC working fluids			Validation cases	
	H_2	O_2	N_2	He	Ar
Mean free path, λ (nm)	121.1	69.3	64.4	190.1	68.5
Kn in GDL	0.002	0.001	0.001	0.003	0.001
Kn in MPL	2.018	1.155	1.073	3.168	1.141

Table 2
Applicability of different flow models in different flow regimes based on Knudsen number [20].

Knudsen number	Flow model
$Kn < 0.001$	Continuum region; Navier–Stokes valid with no-slip boundary condition
$0.001 < Kn < 0.1$	Continuum-transition region; Navier–Stokes valid only with slip boundary condition
$0.1 < Kn < 10$	Transition region; Navier–Stokes not valid, moment equations or Burnett equation with slip boundary condition
$Kn > 10$	Free molecule flow; no continuum model valid

on experimental measurements of absolute permeability in GDLs. Further, among the available open literature, absolute permeability experiments on GDLs and MPL coated GDLs have only been performed using a single working fluid, i.e. nitrogen, air or oxygen [6,8–13]. In the presented results in the literature, permeability values obtained with different working fluids have never been either compared or used to validate predictions from Darcy's law. This is the first goal of this article.

In order to incorporate Knudsen effects to the convective transport in GDLs and MPLs, Kast and Hohenthanner [14] proposed to combine the viscous and Knudsen effects in parallel [14] to obtain a combined resistance. The net transport is then given as the summation of viscous and Knudsen transport. A similar approach has also been proposed by Kerkhof [15] in the binary friction model (BFM) to account for the two modes of transport. The second goal of this article is to experimentally assess the validity of combining viscous and Knudsen effects in parallel, and to develop a methodology to estimate these two parameters.

In this article therefore, the validity of Darcy's model and BFM is studied in detail by developing an experimental setup to measure the pressure drop across a porous media for different mass flow rates and different working fluids. Results show that while the binary friction model (BFM) can reproduce the mass transport losses for all working fluids studied, Darcy's model deviates from the experimental data for gases approaching the transitional regime. Using the BFM model, the article also provides a methodology to estimate both permeability and Knudsen diffusivity of the porous media using the experimental data.

In the following, Section 2 presents the details of the experimental setup and the specifications of the porous media used in this study. Section 3 provides an overview of Darcy's law and BFM, and it explains the data post-processing methods used to extract permeability and Knudsen diffusivities from the experimental data. Finally, Section 4 presents the results obtained using both approaches and their comparison.

2. Experimental setup

To measure the permeability of the porous media, a modified diffusion bridge technique is used [16,17]. The schematics of the permeability measurement experimental setup is shown in Fig. 1. Two flow channels were fabricated in acrylic blocks and meshed together. Silicon gaskets were used in between to separate the channels, except for the place where the GDL connects the flow channels. The porous media is laminated and sealed except for a small aperture made in between where the porous media connects the two flow channels and provides a way for though plane transport in porous media. The inlet of one flow channel and the outlet of the other channel were blocked. This forces the flow to go through the porous media. To control the flow rate across the porous media, a mass flow controller from Cole-Parmer (Quebec, Canada), model: RK-32907-57 with a flow range of 0.5–50 $scm^3\ min^{-1}$ was used. The flow across the porous media produces a pressure drop. The pressure drop was measured by a differential pressure transducer from Omega (Quebec, Canada), customized model: MMDDB10WBIV10H2A0T1A2 of range 0–25 mBar. By varying the flow rate across the porous media, the pressure drop can also be varied. Finally a pressure drop vs flow rate profile can be obtained for the porous media. This profile can be fitted to the porous media flow model to obtain the transport properties.

For experimentation, gas diffusion layers (GDLs) and micro porous layers (MPLs) from the SGL Group were used. Table 3 shows the specifications of the porous media used for experimentation. The MPL coated GDL makes it difficult to analyze the properties of each layer separately. Hence experiments on only GDL were also done to separate the effects of GDL and find transport properties pertinent to the MPL only. For GDL experiments, four layers of SIGRACET 34BA GDL were stacked together and for GDL–MPL experiments, two SIGRACET 34BC were assembled in a mirror image formation, i.e. with the two MPLs facing each other in the

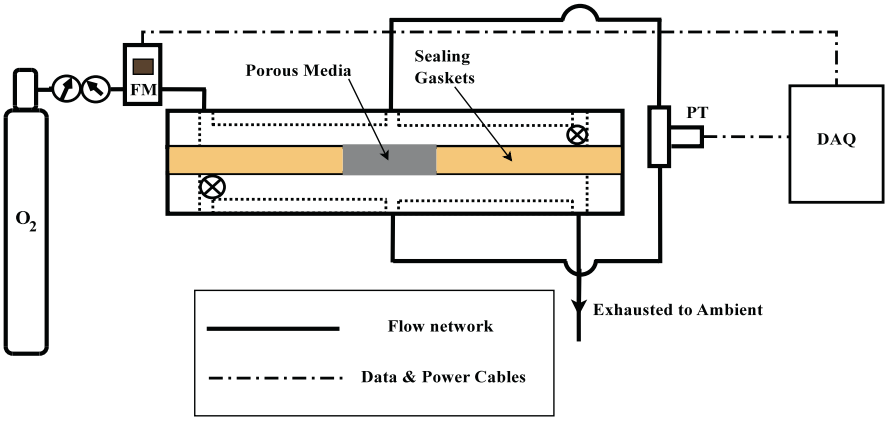

Fig. 1. Schematics of the permeability measurement experimental setup, FM: mass flow controller; PT: differential pressure transducer; DAQ: data acquisition card.

Table 3
Specifications of porous media samples used in experiments.

	GDL only		GDL–MPL	
	Sample 1	Sample 2	Sample 1	Sample 2
Model	SIGRACET 34BA		SIGRACET 34BC	
GDL thickness (μm)	255	251	253	253
MPL thickness (μm)	–	–	64	61
Porosity	83%	83%	75%	75%
PTFE content	5%	5%	5%	5%

interior of the sandwich. The reason for using multiple layers was two fold: (a) to have sufficient pressure drop across porous media, which could be accurately measured by the pressure transducer; and, (b) to ensure that a representative elementary volume of GDL exists [2] since the GDL pore size is of a similar order of magnitude to its thickness (i.e. GDLs contain 60 μm diameter pores in a 250 μm thick layer). The SIGRACET 34 BC has a MPL coated on top of a normal SIGRACET 34 BA GDL. To find the thickness of the MPL in 34BC, the GDL thickness was subtracted from the total thickness. The GDL thickness for the 34 BC was taken as the average thickness from 34 BA measurements. The thickness of the GDLs was measured by a micrometer from Mitutoyo (Japan), Model: CLM1-.6″QM with a constant and adjustable fine-loading device.

To find the repeatability and uncertainty of the experimental data, multiple experiments were done on a GDL–MPL assembly (SGL SIGRACET 34 BC) using oxygen as the working fluid. The maximum margin of error in pressure measurement for a 95% confidence interval was found to be around ±4.5 Pa, for a mean pressure of 1104.7 Pa and a flow rate of 12 $scm^3\ min^{-1}$. The maximum difference between permeability values obtained from these data sets is found to be ±1.7%.

A theoretical error analysis was also done based on the accuracy of different equipments in the experimental setup. The theoretically calculated maximum margin of error is around ±2.5%. This value is within the uncertainty range obtained experimentally.

3. Data estimation methodologies

The permeability measurement setup described in Section 2 is used to obtain the pressure drop across the porous media at different flow rates for different working fluids, e.g. oxygen, nitrogen, helium and argon. The gas flow rate across the porous media is varied by means of a mass flow controller and the corresponding pressure drop is recorded. From experiments, a pressure drop vs flow rate profile is obtained. The velocity across the porous media is obtained by dividing the flow rate with mass transport aperture cross section as follows:

$$v = \frac{\dot{Q}}{\pi D^2/4} \tag{1}$$

where $\dot{Q}$ is the volumetric flow rate of gas across porous media. D is diameter of the porous media aperture, approximately 2 ± 0.1 mm, which is made in the porous media assembly to facilitate mass transport. The diameter is measured using a profilometer (AMBIOS, model: XP-300) for accuracy. Several experiments were performed to guarantee that the size of the aperture did not affect the results.

To estimate the transport properties of the porous media, the experimentally observed pressure vs velocity profiles are fitted to theoretical model predictions. The following section describes two porous media transport models viz. Darcy's model and binary friction model (BFM) for transport property estimation in porous media.

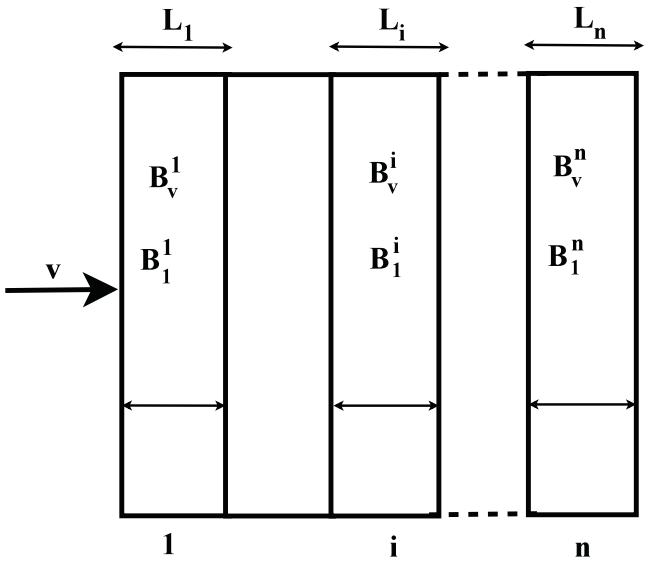

Fig. 2. A schematics of multiple layer assembly in permeability measurement.

3.1. Conventional permeability estimation

Conventionally the pressure gradient vs velocity data is fitted to Darcy's equation given as follows [8]:

$$\frac{dp}{dx} = -\frac{\eta}{B_v} v \tag{2}$$

To account for inertial effects at higher velocities, the Darcy's equations is modified and the Forchheimer term is added to give the Darcy–Forchheimer equation as follows: [9]

$$\frac{dp}{dx} = -\frac{\eta}{B_v} v - \frac{\rho}{B_1} v^2 \tag{3}$$

where B_v and B_1 are the viscous and inertial permeabilities respectively; ρ is the density of the fluid, which is found by using ideal gas law and η is the viscosity of fluid which is estimated from the handbook of Green and Perry [18]. As per the assumptions of Darcy's law in 1-D, the pore average velocity across the porous media can be assumed to be constant [2]. Hence the total pressure variation will be linear. The following equation can be obtained for a single layer of porous media to replace Eq. (3) [9]:

$$\frac{p_1 - p_2}{L} = \frac{\Delta p}{L} = \frac{\eta}{B_v} v + \frac{\rho}{B_1} v^2 \tag{4}$$

where p_1 and p_2 are the pressure values on each side of the porous media. For multiple layers of porous media with varying permeability, the experimental measurement can only obtain effective values of permeability. To know the permeability of each layer exclusively, the effective permeability needs to be separated into its components [9].

Fig. 2 shows an assembly of various porous media with varying permeability values. Neglecting interfacial effects, the total pressure drop across the porous media can be given as follows:

$$\frac{\Delta p}{L} = \frac{\eta}{B_v^{eff}} v + \frac{\rho}{B_1^{eff}} v^2 \Rightarrow \Delta p = \frac{\eta}{B_v^{eff}} L v + \frac{\rho}{B_1^{eff}} L v^2 \tag{5}$$

where B_v^{eff} and B_1^{eff} are the effective viscous and inertial permeability values and L is total thickness. For a single layer of porous media, the equation can be given as follows:

$$\frac{\Delta p_i}{L_i} = \frac{\eta}{B_v^i} v + \frac{\rho}{B_1^i} v^2 \Rightarrow \Delta p_i = \frac{\eta}{B_v^i} L_i v + \frac{\rho}{B_1^i} L_i v^2 \tag{6}$$

where Δp_i is the pressure drop across the ith layer of the porous media, and B_v^i and B_1^i are the viscous and inertial permeability values of the ith layer. Assuming a constant velocity across porous media, the pressure drop across all layers can be summed up as follows [9]:

$$\Delta p = \sum_{i=1}^{n} \Delta p_i = \eta v \sum_{i=1}^{n} \frac{L_i}{B_v^i} + \rho v^2 \sum_{i=1}^{n} \frac{L_i}{B_i^i} \tag{7}$$

where Δp is the total pressure drop across the entire porous media assembly. Comparing Eq. (7) with Eq. (5), the following expressions can be obtained for effective permeability of porous media [9]:

$$\frac{L}{B_v^{eff}} = \sum_{i=1}^{n} \frac{L_i}{B_v^i} \tag{8}$$

$$\frac{L}{B_1^{eff}} = \sum_{i=1}^{n} \frac{L_i}{B_1^i} \tag{9}$$

The effective permeability values can be measured by experimentation on GDL–MPL assemblies. To know the permeability of nth layer, the permeability of other $n-1$ layers must be known. Therefore in case of a GDL–MPL assembly, the GDL permeability has to be estimated in order to obtain the MPL permeability. The parameter of interest in this case is the viscous permeability of the micro porous layer. To find the values of MPL permeability, Eqs. (8) and (9) are used with values of the GDL permeability and the overall permeability. The MPL permeability can be given by the following equation:

$$B_v^{MPL} = L_{MPL} \left(\frac{L}{B_v^{eff}} - \frac{L_{GDL}}{B_v^{GDL}} \right)^{-1} \tag{10}$$

3.2. Permeability and Knudsen diffusivity estimation using BFM

To account for viscous and Knudsen effects together, both transports mechanisms are assumed to be in parallel as previously proposed by Kast and Hohenthanner [14]. The net transport is given as summation of viscous and Knudsen transport as follows:

$$N = -\frac{B_v}{\eta} \frac{dp}{dx} \frac{p}{RT} - D_K^{eff} \frac{1}{RT} \frac{dp}{dx} \tag{11}$$

$$\Rightarrow \frac{dp}{dx} = -RT \left(D_K^{eff} + \frac{B_v}{\eta/p} \right)^{-1} N \tag{12}$$

The above equation can also be obtained by simplifying the binary friction model (BFM) presented by Kerkhof [15]. The BFM is also based on accounting of both viscous as well as wall friction in parallel. For a single species, the interspecies interaction term in BFM vanishes and Eq. (12) is obtained.

While deriving Eq. (11), the effects of inertial permeability are not taken into account explicitly and all non-linear behaviour is attributed to the Knudsen diffusivity. As the non-linear nature can be due to both Knudsen effects as well as inertial effects, the Knudsen diffusivity will behave as a lumped parameter. However in PEMFCs, the Knudsen diffusivity will be the dominant parameter, i.e. the inertial effects are negligible, due to low fluid velocities and small porous media pore radii. As it is shown later in this article, the inertial permeability is not able to account for the non-linear effects for different gases while the Knudsen diffusivity takes into account the non-linearity quite accurately for different gases, highlighting the fact that Knudsen diffusivity is the dominant factor that contributes to the non-linear nature of the pressure vs velocity profiles. Note that for gases like oxygen and nitrogen which have a smaller mean free path, i.e. larger Knudsen number, and thus are in less influence of Knudsen effect in GDL, Darcy–Forchheimer equation should still be used at very high velocities. Micro porous layers will always have higher Knudsen effects than inertial effects unless very high fluid velocities are encountered. As the through-plane velocities in the fuel cell electrodes are usually not very high, neglecting inertial permeability in the BFM approach is a reasonable approach in both GDLs and MPLs.

In the case of a gas diffusion layer, Eq. (12) can be integrated over the length of porous media and the following expression is obtained using the definition of molar fluxes:

$$N = cv = \frac{p}{RT} v \tag{13}$$

$$v = \frac{D_K^{eff}}{L} \ln \left(\frac{p_1}{p_2} \right) + \frac{B_v}{\eta L} (p_1 - p_2) \tag{14}$$

where p_1 and p_2 are the pressure values at the entrance and exit side of the porous media respectively, and L is the total thickness of the GDL assembly.

For the current permeability measurement setup, the gas is always exhausted to ambient pressure ($p_2 = 1$ atm). Hence the velocity is only dependent on p_1. The equation above can be fitted to experimental data for obtaining D_K^{eff} and B_v. The pressure drop is very low in the GDL, therefore the Knudsen term will be almost negligible. Due to the non-linearity of Knudsen term, its sensitivity will be quite high and using both variables as fitting parameter may lead to large errors in estimation of Knudsen diffusivity. As Knudsen diffusion coefficient is inversely proportional to the molecular mass, D_K will be much higher for He. Also as seen in Table 1, the oxygen transport is in the continuum region. Hence for oxygen profile fit, Knudsen diffusivity can be neglected and the Darcy's equation is recovered as follows:

$$v = \frac{B_v}{\eta L} (p_1 - p_2) \tag{15}$$

Once the permeability is obtained from oxygen experimentation, the Knudsen diffusivity can be used as the only fitting parameter with helium experiments.

To measure permeability and Knudsen diffusivity in the MPL, again Eq. (12) can be used. However, fitting data is not as straightforward in MPL, as the experimentation is done for a GDL–MPL assembly. Due to non-linearity of the pressure expression in Eq. (12), separating MPL pressure drop is challenging. Hence in this case numerical modelling is used. The velocity is dependent on permeability and Knudsen diffusivity. To obtain the values of these two parameters the experimentally observed velocity is fitted to the numerical predictions and the following function is minimized:

$$f_{min} = \sum_{i=1}^{n} (v_{exp} - v_{num}(D_K, B_v))^2 \tag{16}$$

where n is the number of data points available for fitting, v_{exp} is the experimentally observed velocity and $v_{num}(D_K, B_v)$ is the estimated velocity as a function of D_K and B_v. To estimate the velocity, Eq. (14) is solved across the GDL and across the MPL by constraining the velocity to be same in both the layers. The system of equations is solved using MATLAB's `fsolve` function and velocity is obtained. The estimated velocity is a function of D_K and B_v. Using MATLAB's `lsqcurvefit` function the experimental data is fitted to the estimation and the values of permeability and Knudsen diffusivity are obtained for best fit. The properties of the GDL are already known and the MPL properties are estimated by fitting the numerical solution to experimental results. As there are two fitting variables (permeability and Knudsen diffusivity), two sets of experimental data are used for simultaneous data fitting.

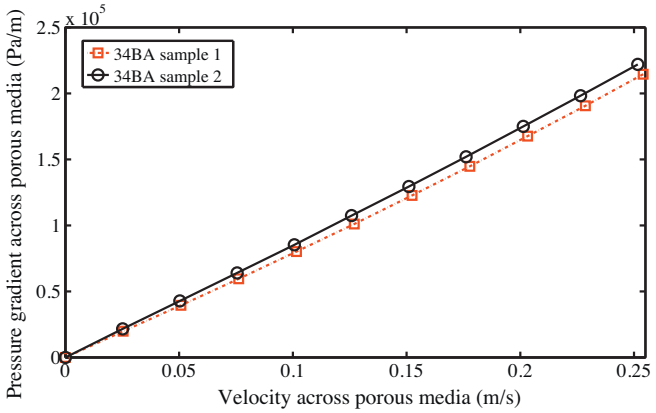

Fig. 3. Pressure gradient vs velocity profiles for two samples of 34BA. Lines represent the data fit and symbols represent the experimental data.

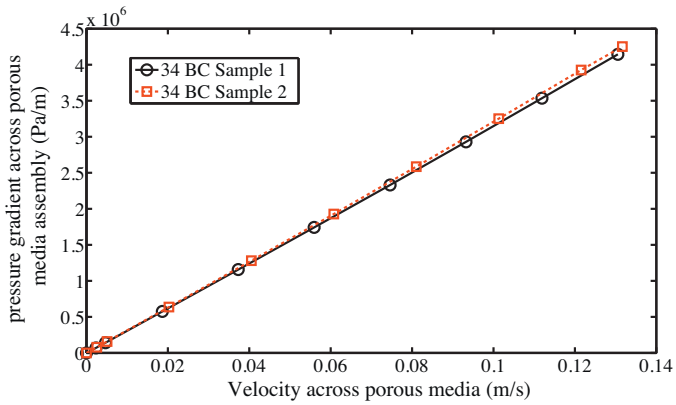

Fig. 4. Net pressure drop vs velocity profile for SGL SIGRACET 34BC assembly. Lines represent the data fit and symbols the experimental data.

Table 4
Permeability values for a SGL SIGRACET 34BA GDL using Darcy–Forchheimer equation.

Parameter	Sample 1	Sample 2	Literature value
Viscous permeability (m^2)	2.74×10^{-11}	2.50×10^{-11}	$1.63 \times 10^{-11} \pm 5.505\,\%$
Inertial permeability (m)	3.61×10^{-6}	6.22×10^{-6}	$\simeq 1.21 \times 10^{-5}$

4. Results

4.1. Permeability results from Darcy's approach

This section describes permeability measurement is SIGRACET GDL and MPL coated GDLs using Darcy–Forchheimer equation for parameter estimation.

4.1.1. Permeability measurements in gas diffusion layers

The pressure gradient vs velocity profile for two SIGRACET 34BA assemblies is shown in Fig. 3 using oxygen as the working fluid. The profile was fitted to Darcy–Forchheimer equation for single layer given by Eq. (4). It can be seen that the Darcy–Forchheimer equation is in good agreement with the experimental data. The maximum error between the datafit and the experimental data is around ±3%. To confirm the reliability of the experimental data, each experiment was repeated 2–6 times. The margin of error in measurements is negligible, so it has not been shown in the figure. To ensure reliability of the results, experiments were also conducted with a second sample of 34BA, and similar results were observed as shown in the same figure. The difference between the two profiles can be attributed to the slight difference in thickness and cross sections of the two samples. In the current experiment, the difference between two different samples is around ≃10%, even though the two samples are from the same sheet of GDL.

Table 4 shows the permeability values for both the samples and their comparison with the earlier results presented by Gostick et al. [8] for SGL SIGRACET 34BA. Comparing with the literature values of Gostick et al. [8], it can be seen that the obtained values have similar order of magnitude but values are quite different. In an other set of experiments, the permeability of two SGL SIGRACET 24BC porous media from different batches was measured. The permeability values are 1.462×10^{-13} m^2 and 5.96×10^{-14} m^2. This shows that there is significant variability between different batches, which can be due to the fabrication uncertainties. The samples used by Gostick et al. [8] were from a different batch than the one used in the current experiment, hence difference in results of similar magnitude to batch variability is observed.

The variation in inertial permeability between samples is much higher. The reason for this is the second order dependence on velocity across porous media. For low velocities, the inertial term will be almost negligible and the associated error will be much higher. The inertial permeability is not used in most mass transport models, so it is not reported in the rest of the article. Also it can be seen from the almost linear nature that the inertial effects are not so significant in GDLs.

4.1.2. Permeability measurements in micro porous layers

A SGL SIGRACET porous media (model: 34BC) was used for experimentation, where the micro porous layer is coated on top of the gas diffusion layer (SIGRACET 34BA). As the permeability values of GDL and MPL are different, the multi layer approach given by Eq. (5) is adopted for estimating MPL permeability. Fig. 4 shows the net pressure gradient vs velocity for the two samples of 34BC assembly using oxygen as the working fluid. The experimental data was fitted to Eq. (5) to get effective permeability values. The maximum error between the Darcy–Forchheimer data fit and experimental values is around ±2.8%. The experiments on two samples also confirm the reliability of the data. Table 5 shows the permeability values for both samples and their comparison with results presented by Gurau et al. [9]. The viscous and inertial permeability values for both samples are close to each other, confirming the reliability of the experiment.

It should be noted that Gurau et al. [9] in their permeability measurements on GDL–MPL assemblies have used a different porous media which had 30% PTFE coating compared to 5% PTFE coating in SIGRACET 34BC. Their experimental data have been only used as a reference and to confirm that the permeability values obtained in current experiment are of similar order of magnitude.

Table 6 shows the permeability values for different layers obtained from experiments. The MPL permeability values calculated by Eq. (10) are also shown in the table. To find the MPL only permeability values in 34BC, average properties of both 34BA experiments were used for GDL. It can be seen that the MPL

Table 5
Permeability values for a SGL SIGRACET 34BC GDL–MPL assembly using Darcy–Forchheimer equation.

Parameter	Sample 1	Sample 2	Literature value
Viscous permeability (m^2)	6.73×10^{-13}	6.61×10^{-13}	$4.4 \times 10^{-13} - 7.9 \times 10^{-13}$
Inertial permeability (m)	1.57×10^{-7}	1.59×10^{-7}	$0.63 \times 10^{-7} - 3.4 \times 10^{-7}$

Table 6
Permeability calculations for a SGL SIGRACET 34BC GDL–MPL assembly using Darcy–Forchheimer equation.

Parameter	Sample 1	Sample 2
GDL permeability (m^2)	2.62×10^{-11}	2.62×10^{-11}
MPL permeability (m^2)	1.39×10^{-13}	1.31×10^{-13}
Overall (34BC) permeability (m^2)	6.73×10^{-13}	6.61×10^{-13}

permeability values are two orders of magnitude less than the GDL permeability. Due to such low permeability, the MPL becomes the convective transport limiting layer in this assembly. The layer specific permeability values can be used for better modelling of convective transport in GDL–MPL assemblies.

4.1.3. Darcy's law validation

Using the Darcy–Forchheimer equation, it has been shown that the estimated permeability values are similar to the values obtained earlier by other researchers. However the continuum assumption on which the Darcy's law is based, breaks down at small pore sizes. To verify the deviation from Darcy's law at high Knudsen numbers, further permeability experiments on the SGL SIGRACET34 BA GDL were done with helium. The permeability values obtained earlier with oxygen, as shown in Table 4 were used for comparisons. The difference between permeability values in both experiments is around ±8%. As shown in Table 1, the helium flow in the GDL is in transition region. The molecular weight of helium is less than oxygen, which will results in helium having a higher Knudsen diffusivity. Since in the transition region, the effects of Knudsen transport will be present which are not accounted by Darcy's law, there is a difference between the experimental and predicted pressure drop values.

In the MPL, the error will be even larger as the molecule wall collision will become more dominant and viscous effects will start diminishing. Fig. 5 shows the difference between observed and predicted pressure drop values across a 34BC assembly for helium and nitrogen flow. The maximum difference between the experimental and predicted values is around 10% for helium and 3% for nitrogen. The difference between slopes of the curves is higher for 34BC compared to 34BA, which indicates a higher difference between actual and predicted permeability values. Helium has a much higher Knudsen diffusivity than oxygen, hence the pressure drop due to Knudsen effects will be less. Therefore, the pressure drop in helium experiments is less than the values predicted by oxygen experiments. In case of nitrogen the Knudsen diffusivity is very similar to that of oxygen and hence the predictions are quite close to experimental data. It can be seen that the Darcy–Forchheimer

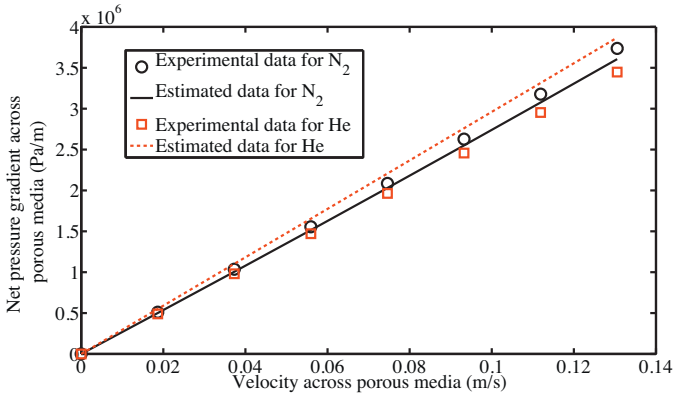

Fig. 5. Comparison of experimentally observed pressure drop across a SGL SIGRACET 34BC GDL–MPL assembly with Darcy–Forchheimer prediction.

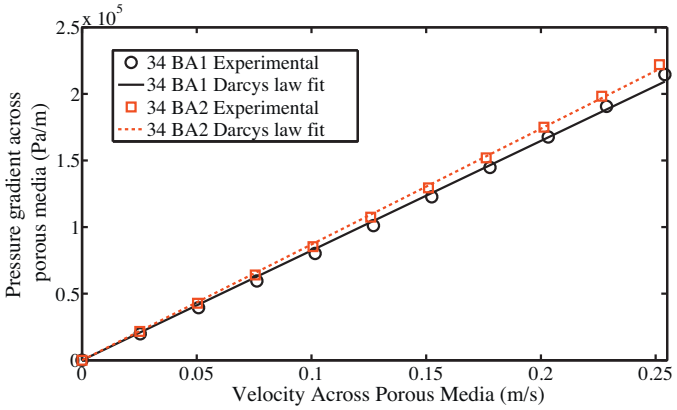

Fig. 6. Experimental results vs Darcy's datafit for O_2 in a SGL SIGRACET 34BA GDL.

equation is not able to take into account the varying effects between different gases when Knudsen effects are important.

4.2. Permeability and Knudsen diffusivity results using BFM

As shown in Section 4.1.3, Darcy's law is not able to predict convective transport for different gases. This section presents viscous permeability and effective Knudsen diffusivity estimation in GDLs and MPL coated GDLs using the binary friction model for parameter estimation.

4.2.1. Permeability and Knudsen diffusivity estimation in GDL

As discussed in Section 3.2, the oxygen flow in GDL flow is assumed to be in continuum region and Darcy's law is used for permeability estimation using Eq. (15). Fig. 6 shows the comparison of experimental observations with Darcy's model datafit for two samples of SIGRACET 34BA. The viscous permeability values of the two samples of SIGRACET 34BA GDL is around 2.51×10^{-11} m^2 and 2.37×10^{-11} m^2, with maximum error in data fit being around ±6%. As the Darcy's law is unable to incorporate the nonlinearity of the transport, the fitting errors are slightly high compared to a non-linear model. However the linear fit is only used to predict the viscous permeability, which is the dominant and linear parameter for oxygen transport. The non-linear behaviour is attributed to the Knudsen effects which are found as follows.

The average viscous permeability of SIGRACET 34 BA GDL is used in the next stage of data processing. Using this value of permeability, Eq. (14) is fitted to the data obtained with helium experimentation. Fig. 7 shows the comparison of experimental results with BFM datafit. As p_1 is the independent variable, it is used as the x-axis parameter. The permeability is already known

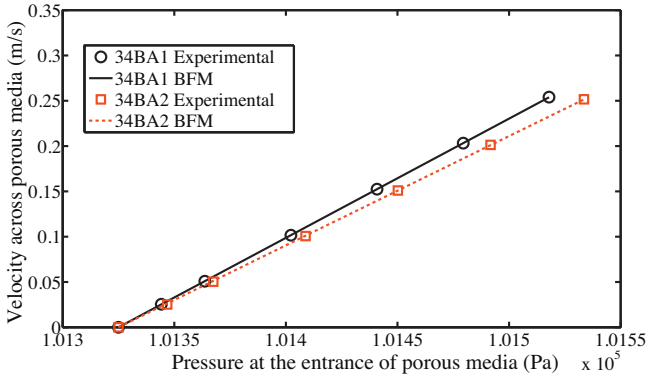

Fig. 7. Experimental results vs BFM datafit for *He* in a SGL SIGRACET 34BA GDL.

Table 7
Transport properties of SIGRACET 34 BC PEM fuel cell porous media using binary friction model.

Parameter	GDL	MPL
Viscous permeability, B_v (m^2)	2.44×10^{-11}	1.247×10^{-13}
Knudsen diffusivity (He), $D^{eff}_{K,He}$ ($m^2\,s^{-1}$)	4.632×10^{-3}	9.35×10^{-5}
Knudsen diffusivity (O_2), D^{eff}_{K,O_2} ($m^2\,s^{-1}$)	1.638×10^{-3}	3.3×10^{-5}

from oxygen analysis and Knudsen diffusivity is used as a fitting parameter. The Knudsen diffusivity for helium in the GDL is around $7.654 \times 10^{-3}\,m^2\,s^{-1}$ and $1.612 \times 10^{-3}\,m^2\,s^{-1}$ for the two samples. The experimental results show excellent agreement with the trend of theoretical model. For verification, the effective pore radius r_p^{eff} can be obtained from the effective Knudsen diffusivity as follows:

$$D_K^{eff} = 0.89 \times \frac{2}{3} r_p^{eff} \left(\frac{8RT}{\pi M}\right)^{1/2} \quad (17)$$

The average effective pore radius for SIGRACET 34BA is found to be around 6.2 μm. This value is within the range of pore size distribution (1–150 μm) for gas diffusion layers [5,6]. This provides a partial validation to the idea of using binary friction model for estimating flow in porous media. Further validation can be done by using other gases of different molecular weights (see Section 4.2.3).

4.2.2. Permeability and Knudsen diffusivity estimation in MPL

The experimental data on SIGRACET 34BC GDL–MPL assembly was fitted to the numerical solution of Eq. (12) for the permeability and Knudsen diffusivity of the MPL. By using a least square parameter estimation permeability and effective Knudsen diffusivity of the MPL were obtained. Table 7 shows the average permeability and effective Knudsen diffusivity in GDL and MPL of a SIGRACET 34BC porous media obtained using the BFM approach. The permeability values are slightly smaller than the ones obtained by Darcy–Forchheimer equation (see Table 6), due to accounting for Knudsen flow. The Knudsen diffusivity values in MPL are around two orders of magnitude less than in GDL, which is in the acceptable range. The use of BFM helped in accounting for the Knudsen transport through nano pores of the porous media and in turn helped in reducing the error in transport properties estimation.

For partial validation of Knudsen diffusivity in MPL, the effective pore radius can be calculated using Eq. (17). For the SIGRACET 34BC MPL the average effective pore radius is found to be 125 nm. The calculated value is within the range of pore size distribution in MPL [5,7].

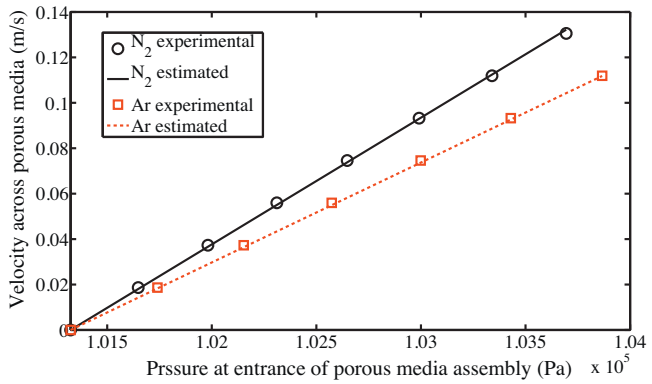

Fig. 8. Comparison of experimental and BFM predictions for flow across a SGL SIGRACET 34 BC.

4.2.3. Binary friction model validation

To validate the applicability of binary friction model (BFM), two validation experiments were carried out with nitrogen and argon on a sample of SIGRACET 34BC. The theoretical estimate of velocity across the GDL–MPL assembly is obtained by numerical solution of Eq. (12). The parameters provided in Table 7 were used for theoretical estimation. Fig. 8 shows the comparison of experimental and theoretical predictions of velocity across the porous assembly. The difference between the experimental and theoretical results for nitrogen is around ±3.5% and for argon is around ±2.5%. It can be seen that the BFM predicts the flow in porous media with better accuracy than the Darcy–Forchheimer equation. This analysis shows that the Knudsen transport is significant in fuel cell porous media, and must be taken into account for accurate predictions.

5. Conclusion

The absolute gas permeability, inertial permeability and effective Knudsen diffusivity of SGL SIGRACET 34BA and 34BC gas diffusion layers and micro porous layers were measured experimentally using a permeability setup inspired on a diffusion bridge setup. The experimental results show that Darcy's law is not capable of accurately predicting the transport, especially in MPLs due to Knudsen effects. A new approach based on the binary friction model was presented to account for viscous and Knudsen transport simultaneously. The use of BFM provides a way to estimate viscous permeability as well as effective Knudsen diffusivity of the porous media. In the continuum region, Darcy–Forchheimer equation should be used at high velocities, e.g. oxygen and nitrogen flow in GDL. However in the transitional regime; e.g. flow in MPLs and hydrogen or helium flow in GDLs, experimental validation of the models show that the BFM is capable of predicting transport with much higher accuracy than the conventional Darcy's model.

Acknowledgements

The authors would like to thank University of Alberta and the Natural Science and Engineering Research Council of Canada for financial assistance. The authors would also like to acknowledge RR Gilpin memorial scholarship for financial assistance.

References

[1] M.A. Van Doormaal, J.G. Pharoah, International Journal for Numerical Methods in Fluids 59 (1) (2009) 75–89.
[2] S. Whitaker, Transport in Porous Media 1 (1) (1986) 3–25.
[3] W.G. Gray, K. O'Neill, Water Resources Research 12 (2) (1976) 148–154.
[4] H. Teng, T. Zhao, Chemical Engineering Science 55 (14) (2000) 2727–2735.
[5] M. Martinez, S. Shimpalee, J.V. Zee, A. Sakars, Journal of the Electrochemical Society 156 (5) (2009) B558–B564.
[6] M. Williams, E. Begg, L. Bonville, H. Kunz, J. Fenton, Journal of the Electrochemical Society 151 (8) (2004) A1173–A1180.
[7] S. Thiele, R. Zengerle, C. Ziegler, Nano Research (2011) 1–12.
[8] J. Gostick, M. Fowler, M. Pritzker, M. Ioannidis, L. Behra, Journal of Power Sources 162 (1) (2006) 228–238.
[9] V. Gurau, M. Bluemle, E.D. Castro, Y.-M. Tsou, T. Zawodzinski Jr., J. Mann Jr., Journal of Power Sources 165 (2) (2007) 793–802.
[10] J. Ihonen, M. Mikkola, G. Lindbergh, Journal of the Electrochemical Society 151 (8) (2004) A1152–A1161.
[11] M. Prasanna, H. Ha, E. Cho, S.-A. Hong, I.-H. Oh, Journal of Power Sources 131 (1–2) (2004) 147–154.

[12] M. Ismail, T. Damjanovic, K. Hughes, D. Ingham, L. Ma, M. Pourkashanian, M. Rosli, Journal of Fuel Cell Science and Technology 7 (5) (2010) 0510161–0510167.
[13] M. Ismail, D. Borman, T. Damjanovic, D. Ingham, M. Pourkashanian, International Journal of Hydrogen Energy 36 (16) (2011) 10392–10402.
[14] W. Kast, C.-R. Hohenthanner, International Journal of Heat and Mass Transfer 43 (5) (2000) 807–823.
[15] P. Kerkhof, Chemical Engineering Journal and the Biochemical Engineering Journal 64 (3) (1996) 319–343.
[16] T. Marrero, E. Mason, Journal of Physical and Chemical Reference Data 1 (1) (1972) 3–118.
[17] L.M. Pant, S.K. Mitra, M. Secanell, ASME 2011 9th International Conference on Nanochannels, Microchannels, and Minichannels, no. ICNMM2011-58181, Edmonton, Alberta, Canada, 2011.
[18] D. Green, R.H. Perry, Perry's Chemical Engineers Handbook, 8th edition, Mcgraw-Hill, 2008.
[19] J. Hirschfelder, C. Curtiss, R. Bird, Molecular Theory of Gases and Liquids, Wiley, 1954.
[20] R. Agarwal, K.-Y. Yun, R. Balakrishnan, Physics of Fluids 13 (10) (2001) 3061–3085.